

EMBEDMENT EFFECTS BY FORCED VIBRATION TESTS AND ANALYSIS OF A LARGE-SCALE BUILDING MODEL ON THE ACTUAL GROUND

Tetsuo Abiru, Takashi Hashimoto & Etsushi Ochiai

Chugoku Electric Power Co., Inc., Japan

Hiroyuki Sugita, Yasutsugu Suzuki, Kenji Iwamoto, Hiroya Murakami

Kajima Corporation, Japan



SUMMARY:

The forced vibration tests and the simulation analyses were performed for a large-scale building model of an RC structure constructed on the actual ground. Using the embedment soil conditions as parameters, the following findings were obtained, through the limited cases of study, for the embedment effects: 1) the displacement amplitude on the roof level of the embedded building model decreases less than half of that of the building model without embedment. 2) The response characteristics are almost the same, even when the width of MMR, a backfill material surrounding the model, is reduced from twice the foundation width of the building model to 2/3 of such width. 3) The response characteristics obtained by the tests can be reproduced by the simulation analyses in which the thin-layer model method and the 3-D FEM are combined for the surrounding soil, and the embedment effects can be evaluated using such an analysis model.

Keywords: Embedment effects, Exciter, Large-scale Building Model, Simulation Analysis, Soil Improvement

1. INTRODUCTION

In a seismic design for a reactor building of a nuclear power plant, the embedment effects of soil around the building are taken into account. Meanwhile, it is a common practice to use Novak's soil springs in a seismic response analysis where surrounding soil is assumed to be a semi-infinite body, however, the actual surrounding soil of the building is a finite body. Previous studies on the embedment effects (c.f. Sitharam 2005¹) the relationship of the range of soil improvement and the embedment effect is not clarified.

While seismic observation of the building model constructed on the actual ground² or the forced vibration test using the exciter³ is considered to be an effective method to solve such embedment effects, no study was found that investigated the effects of embedment range by soil improvement. Furthermore, a building vibration tests on the actual ground are usually performed with a rigid structure, but the flexibility of the structure was also considered in this study.

Accordingly in this report, the forced vibration tests using the exciter were performed for a large-scale building model of RC structure on the actual ground using backfill conditions as parameters. And, also a simulation analyses of the building model using a hybrid model of the 3-D FEM and thin layer element method for the soil were conducted. It was confirmed from the test results that the embedment effects can be obtained even when the range of soil improvement around the building was limited, and the embedment effects were able to be effectively represented by the analysis.

2. OUTLINE OF VIBRATION TEST

2.1 Test Cases

The outline of the test model is shown in Figure 1, and the test cases are shown in Table 1. The size of the building model is 8 m square and the height is 7 m (three-story structure). Three test cases were considered to obtain data for the embedment effects. Case 1 is a Non-embedded model. Case 2 is a model with MMR (lean mix cement treated soil) backfill 1/3 of the height of the building model and as

far as to twice the width D of the building model. And Case 3 is a model where the outside area of MMR taken away and hilled with the improved soil (compacted crusher run, which is softer than MMR). Photo 1 shows the state of the building model and the surrounding soil in Case 1.

The test ground was excavated to a depth of 5 m within the square area having each side of 40 m, which is five times the width D of the building model (8 m). The forced vibration test for Case 1 was conducted by the exciter installed on the roof. Next, the surrounding ground of the building model was backfilled to a depth of 2.5 m with MMR, and the forced vibration test for Case 2 was conducted. After the Case 2 test, MMR at the outside was replaced with the improved soil. The forced vibration test for Case 3 was conducted in this condition. After Case 3 test, an additional vibration test using the large exciter was also conducted.

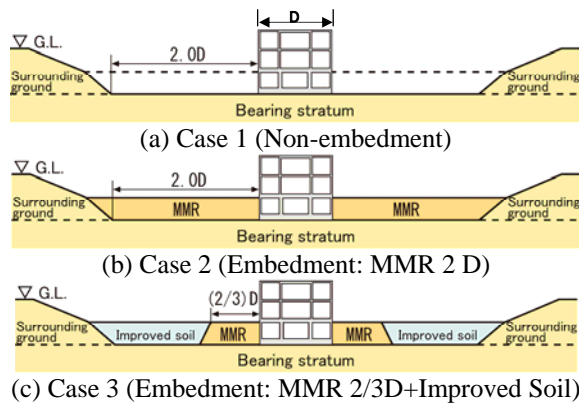


Photo 1 General View of Building Model and Surrounding Soils (Case 1)

Figure 1 Test Models

Table 1 Test Cases

Case	Test name	Test condition					Embedment condition
		Exciter	Force	Position	Direction	Frequency	
Case1	C1-RX	Small Exciter	9.8 kN	RF	X ^{*1}	2–30Hz	Non-Embedded
	C1-RY				Y ^{*2}		
Case2	C2-RX				X ^{*1}		Embedded by MMR(2 D)
	C2-RY				Y ^{*2}		
Case3	C3-RX				X ^{*1}		Embedded by MMR(2/3 D) +Improved soil
	C3-RY				Y ^{*2}		
Intensive excitation test	L-2	Large Exciter	19.6 kN	X ^{*1}	2–20Hz		
	L-5		49.0kN				
	L-10		98.0 kN				

*1) Direction of flexible structure

*2) Direction of rigid structure

2.2 Design of The Building Model and The Soil

The law of similarities between the actual building considered and the model building is as shown in Table 2. The similitude ratio is established by the dimensional analysis so that the ratio of dimensionless frequency becomes 1.0 with length L , time T , and density ρ as fundamental quantities because the density and the gravitational acceleration are unchangeable. The target values and the measured values of the model that were determined by the actual building considered and by the law of similarities are shown in Table 3. The target value for shear wave velocity of the surrounding ground is 40 m/s based on the law of similarities, but this value is difficult to realize. Yet, the analysis indicates that the effect of the shear wave velocity on the surrounding soil is small at a point more than $2D$ in distance from the building. The other properties were generally close to the target values.

Figure 2 shows how the ground was excavated. A slope was provided in one direction for construction work. The plan view of the building model is shown in Figure 3, and the cross section is shown in Figure 4. The model was designed as a flexible building model having a frame structure in the X-direction and as a rigid building model having a shear wall structure in the Y-direction. Accordingly, shear walls were provided also inside the building model in addition to the periphery in the

Y-direction. The periphery of the basement was required to be enclosed by walls because of soil pressure caused by the backfilled soil, but the stiffness of the structure would increase too much as the flexible building model. So slits in the letter H shape were provided in the underground walls in the X-direction to reduce shear stiffness as shown in Photo 2. Two floor openings for the access of personnel and equipments were located on each floor at the symmetrical locations. As such, the building model was designed to be perfectly symmetrical in the X and Y directions so that no torsional motion of the structure could be produced.

Table 2 Law of Similarity Between Actual Building Considered and Building Model

Physical value	Symbol	Dimension	Model/Actual building	Actual building	Model
Non-dimensional Frequency	$a_0 = \omega \sqrt{A/Vs}$	Non	1	-	-
Length (Displacement)	L	L	1/10	Width 80 m	Width 8 m
Density	ρ	$\rho (=M/L^3)$	1	RC:2.4 g/cm ³	RC:2.4g/cm ³
Mass	M	ρL^3	1/1000	-	-
Gravity acceleration	g	g (=L/T ²)	1	-	-
Time	T	T	1/2	-	-
Vs(Bearing stratum)	V	L/T	1/5	2000 m/s	400 m/s
Horizontal acceleration	α	L/T ²	1/2.5	-	-
Frequency	f	1/T	2	0–15 Hz	0–30 Hz

Table 3 Comparison Between Values of Actual Building Considered and Target and Actual Values of Building Model

	Physical value	Actual building	Model		
			Target	Result	Result/Target
Building	Width	80 m	8 m	8 m	1.00
	Height	65 m	6.5 m	7 m	1.08
	Depth of embedment	20 m	2.0 m	2.5 m	1.25
Bearing stratum	Vs	2000 m/s	400 m/s	275–378 m/s	0.69–0.95
MMR	Vs	1500 m/s	300 m/s	243–257 m/s	0.81–0.86
Improved soil	Vs	700 m/s	140 m/s	167 m/s	1.19
Surrounding ground	Vs	200 m/s	40 m/s	282 m/s	7.05

2.3 Layout of Sensors

Figure 2 shows the location of the sensors in the soil, and Figures 3 and 4 show the location of the sensors of the building model. The exciter was installed on the roof of the building model in the center, and vibration tests in the X- and Y-directions were conducted, changing the direction of the exciter. The same arrangement of sensors (servo type velocity meter) was used for both excitation directions. For the soil, sensors with three components were installed at three points in each of four directions from the center of the building model. The outermost sensors were located on the ground not excavated. At 5 or 8 points on each floor level of the building model, sensors for the horizontal two components were installed, and sensors for the vertical component were installed in four corners on each floor level and in four positions in the center of the roof and the basement floor.

2.4 Vibration Test Method and Data Processing Method

The forced vibration tests for Cases 1, 2, and 3 were conducted using the small exciter in the frequency range between 2 and 30 Hz increasing the frequency by 0.1 or 0.2 Hz steps. At each frequency, time history data for 100 waves were obtained, and the exciting frequency, velocity amplitude, and phase lag from the exciting force were measured by the cross-correlation function with the rotational signal of the exciter. While the amplitude obtained was velocity, it was converted into displacement and further normalized as displacement for 1 kN of exciting force. The maximum exciting force of the small exciter was 9.8 kN, but as it was a type to produce exciting force by rotating a weight of a constant mass, the exciting force increased as the frequency increased, and a maximum of 9.8 kN could be obtained at a frequency of about 22 Hz. When the maximum exciting

force was reached, the eccentric mass of the weight was reduced to continue the test at a higher frequency for the next step. As such, the excitation force was not constant throughout the test, but it was generally within the range of an elastic response, and no discontinuous steps were observed before and after the weight changed. On the other hand, because the large exciter was the type where an eccentric mass could be automatically changed while the weight was rotating, a constant exciting force of 98.0 kN was maintained in the frequency range of 2–20 Hz, and used in the intensive excitation tests at exciting forces of 19.6 kN, 49.0 kN, and 98.0 kN, respectively.

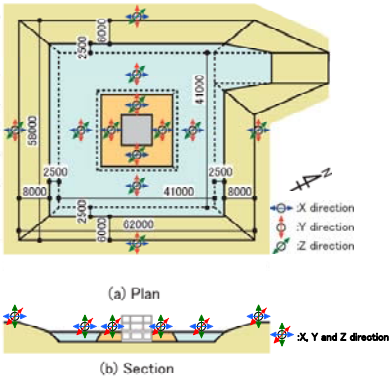


Figure 2 Excavation Geometry of the Soil and Layout of Sensors on Soils



Photo 2 Building Model and H-shaped Slits in Underground Wall

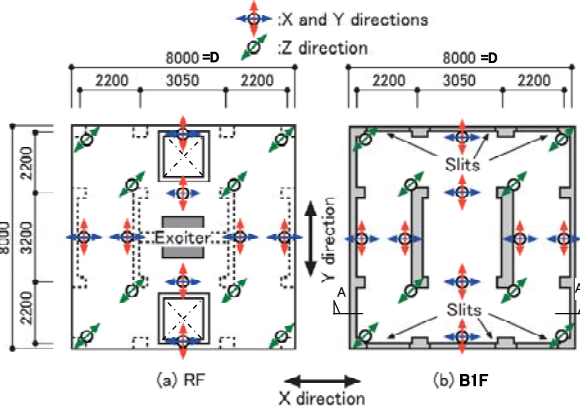


Figure 3 Building Model Plan View and Locations of Exciter and Sensors

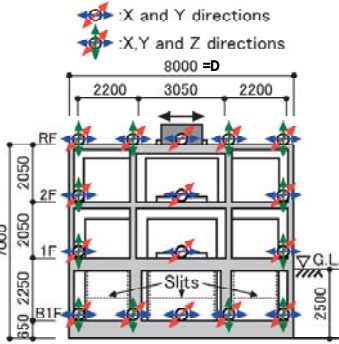


Figure 4 Building Model Sectional View and Locations of Exciter and Sensors (X-X' Section)

3. RESULTS OF VIBRATION TESTS

3.1 Resonance Curves and Phase Lag Curves

The resonance curves and phase lag curves obtained on each floor level in the forced vibration tests of Cases 1 through 3 with respect to X-direction excitation are shown in Figure 5 and in Figure 6 with respect to Y-direction excitation. The primary resonant amplitude was observed at 8.9 Hz in the X-direction excitation of Case 1, and it was shown that the amplitude of the primary mode increased as the floor level increased. In Cases 2 and 3, the primary resonant amplitudes were observed almost at the same frequencies of 15.7 Hz and 16.2 Hz respectively, and the normalized amplitude was reduced to less than half of the amplitude observed in Case 1 (Case2:0.39, Case3:0.46). In all three cases, the phase lag observed on the roof near the primary resonant amplitude frequency passed 90 degrees, and the peak could also be identified by the phase lag.

On the other hand in Case 1, the primary resonant frequency in the Y-direction was at 10.4 Hz, and the same as in the X-direction, the amplitude of the primary mode increased on the upper floor level. In Cases 2 and 3, identification of the primary resonant amplitude was difficult due to so many smaller peaks, but using the position where the phase lag on the roof crossed 90 degrees, the same as in the case of the X-direction for identification of the primary resonant amplitude, almost the same 16.7 Hz

and 16.9 Hz were identified as the primary resonant amplitude in the respective cases, and furthermore, the normalized amplitude reduced less than a quarter of the value in Case 1 (Case2:0.24, Case3:0.22). In Case 2, another peak was observed at 12.4 Hz, which was lower than the 16.7 Hz identified as the primary resonant amplitude. A small peak was observed near this frequency in the X-direction of the same Case 2 and in Case 3, while the amplitude of the peak was much smaller. While it is estimated that these small peaks were generated due to the effect of the reflected wave from the hard soil at large depth, it was difficult to confirm from the test results.

Resonance curves and phase lag curves obtained by fitting the resonance curve with the response of a point mass are indicated in the graphs as black solid lines, and the resonant frequencies and damping factors are shown in Table 4 and in the graphs. A damping factor is evaluated as 13%–14% in Case 1 and 12%–23% in Cases 2 and 3, which indicates that the damping factor tends to increase by embedment.

As shown in these results, it is clear that amplitude in Cases 2 and 3 with embedment is smaller than the amplitude in Case 1 without embedment, which indicates the effect of the embedment. It was also shown that the response characteristics were almost the same both in Case 2 where the backfilled soil was MMR (2 D) and in Case 3 where the backfilled soil was MMR (2/3 D) + Improved Soil.

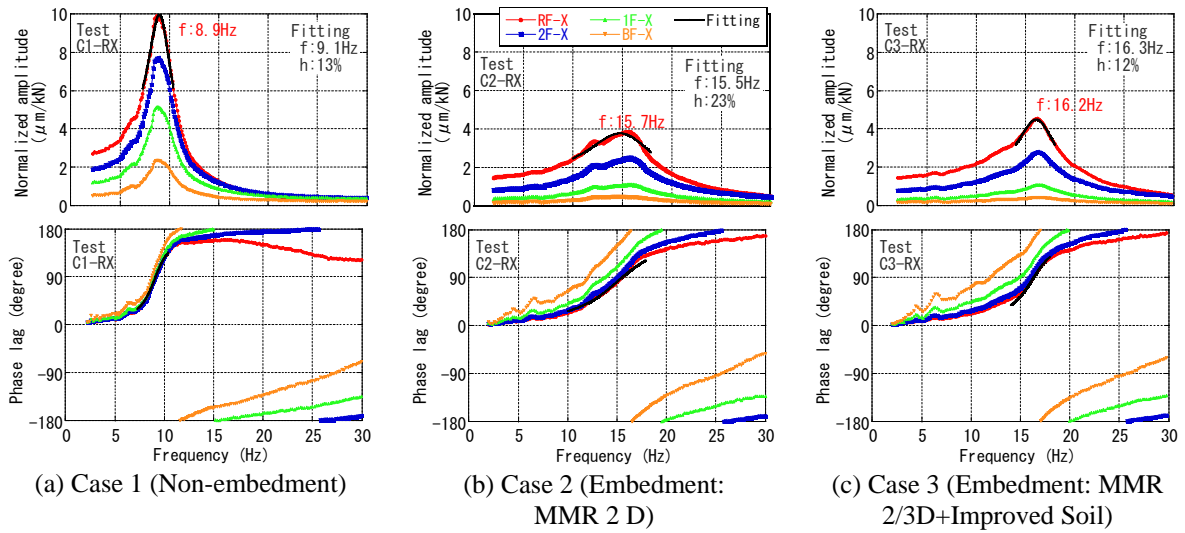


Figure 5 Resonance Curves and Phase Lag Curves in X-direction Excitation on the Roof

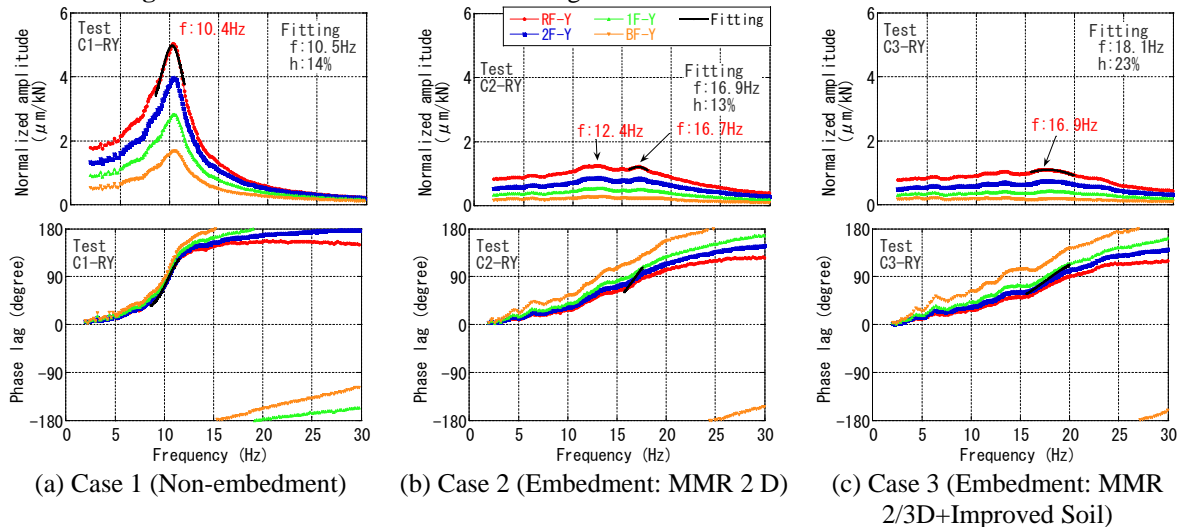
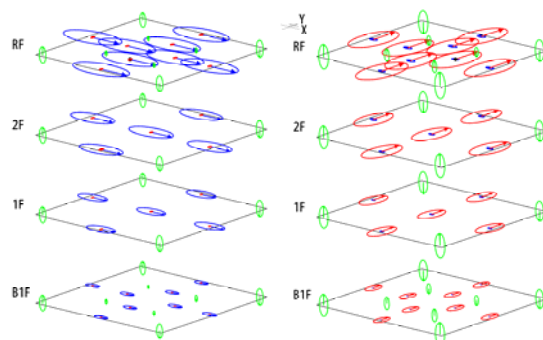


Figure 6 Resonance Curves and Phase Lag Curves in Y-direction Excitation on the Roof

3.2 Vibration Mode

Figure 7 shows the diagrams of primary resonance mode of Case 1. Ellipses in the diagram indicate amplitudes in the respective directions (Blue: X-, Red: Y-, and Green: Vertical directions), and the direction of the arrow shows the phase lag from the reference point.

It is shown that in the X-direction, the sizes of the blue ellipse and the directions of the arrows on all the floor levels agree very well, the red ellipses in the orthogonal direction are very small, and the green ellipses in the vertical direction are in the same size, and the direction of the arrows changed by 180 degrees in front of and behind the exciter. This means that it is a horizontal vibration mode, including a rocking motion without any torsional mode. It is also the same in the Y-direction, and a very clear vibration mode can be observed.



(a) X-direction:8.9Hz (b) Y-direction:10.4Hz
Figure 7 Vibration Mode Diagram in Primary Resonance (Case 1: Non-embedment)

4. OUTLINE OF ANALYSES

Simulation analyses were conducted for the six forced vibration tests shown in Figures 5 and 6. The analysis model, properties of the building model, and properties of the soil used in the analyses are shown in Figure 8, Table 4, and Table 5 respectively. In order to make an accurate evaluation of the interaction between the building structure and the soil, the soil was represented using a combination of the thin layer element method and 3-D FEM. The building model was represented by the lumped mass system having bending and shear stiffness, and the simulation model was constructed combined with the soil model. The properties of the building model used in the study were determined based on the design model and the results of strength tests of concrete, and the properties of the soil model used in the study were determined based on the results of the P-S logging investigation and the surface wave survey conducted at the test site.

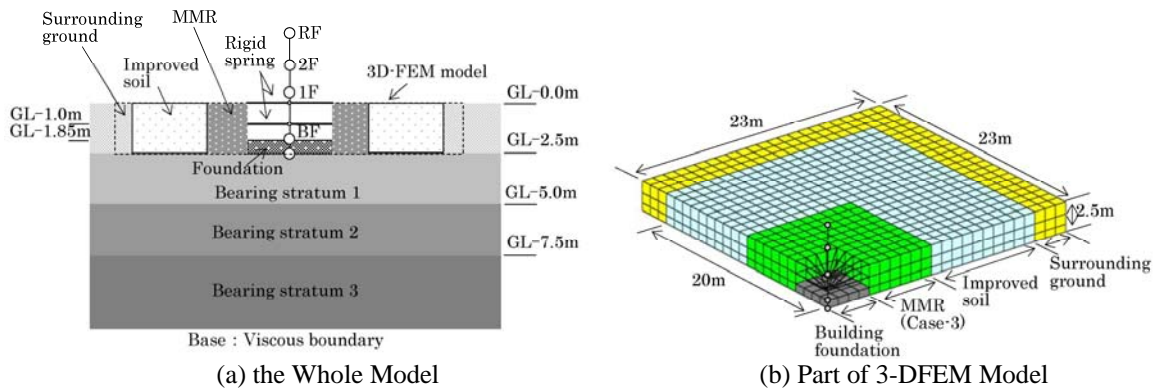
In Case 1, the soil model was represented using the thin layer element method, and the building structure was represented by the lumped mass system having bending and shear rigidity, and they were combined as the analysis model. In Cases 2 and 3, because it was necessary to take the effect of the surrounding MMR and the improved soil into consideration, the model for the portion of the improved soil was made using 3-D FEM, and it was combined with the thin layer element method based on the flexible volume method. In order to take the embedment condition, rigid springs were assumed between the center of the building structure and the point where the structure and the soil were in contact at each depth of the soil. In Case 2 and 3, 1/4 symmetrical condition for analysis was introduced because of symmetry of test model. A frequency response analysis was made changing the frequency at 0.2 Hz intervals, and the unit exciting force was applied at the node where the exciter was placed in the test, and the response of each node was analyzed and compared with the results of the vibration test.

Table 4 Summary of Analysis Properties: Building Model

Position	Height (G.L.+m)	Weight	Rotational inertia	Sectional area		Moment of second order	
				X	Y	X	Y
RF	4.50	430 kN	2294 kNm ²				
2F	2.45	684 kN	3659 kNm ²	0.2512 m ²	2.88 m ²	∞	5.58 m ⁴
1F	0.40	1035 kN	5557 kNm ²	0.3891 m ²	4.64 m ²	∞	29.6 m ⁴
BF	-1.85	780 kN	4179 kNm ²	0.5992 m ²	6.08 m ²	∞	30.3 m ⁴
Bottom	-2.50	499 kN	2667 kNm ²	64.0 m ²	64.0 m ²	341.3 m ⁴	341.3 m ⁴

Table 5 Summary of Analysis Properties: Soils

Soil name	Thickness	Wet density	Shear wave velocity	Poisson's ratio	Damping factor
Surrounding ground	2.5 m	1.80 g/cm ³	282 m/s	0.34	5 %
MMR(Case2)	2.5 m	1.87 g/cm ³	243 m/s	0.32	4 %
MMR(Case3)	2.5 m	1.87 g/cm ³	257 m/s	0.32	5 %
Improved soil	2.5 m	1.87 g/cm ³	167 m/s	0.36	7 %
Bearing stratum 1	2.5 m	1.80 g/cm ³	275 m/s	0.37	5 %
Bearing stratum 2	2.5 m	1.80 g/cm ³	279 m/s	0.38	5 %
Bearing stratum 3	∞	1.80 g/cm ³	378 m/s	0.37	5 %

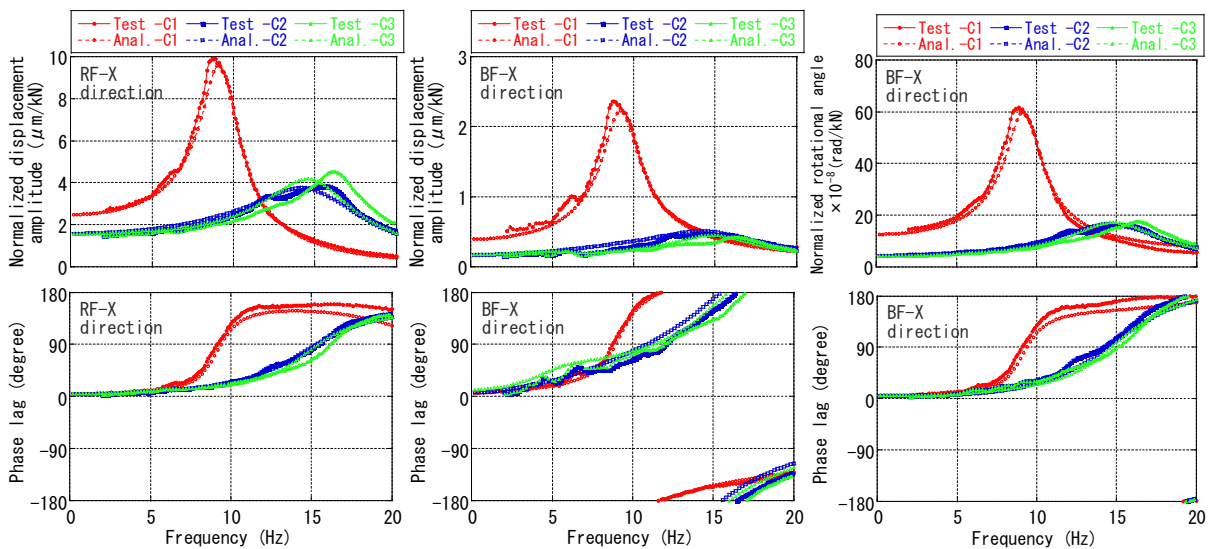


(a) the Whole Model (b) Part of 3-DFEM Model
Figure 8 General Description of Analysis Model (Case 3)

5. COMPARISON OF TEST RESULTS AND ANALYSIS RESULTS

5.1 Resonance Curve and Phase Lag Curve

Figure 9 (excitation in X-direction) show the resonance curves and phase lag curves obtained from the results of simulation analyses of the six forced vibration tests shown in Figures 5 and 6 compared with the test results. In both Figures 9, (a) shows comparison of the resonance curves and phase lag curves in horizontal displacement by excitation on the roof, (b) shows the same comparison in horizontal displacement in the basement, and (c) shows the same comparison in the basement rotational angle in Cases 1,2, and 3. The rotational angle was calculated by the vertical displacement measured at four corners in the basement and the distance between sensors. The test results and the analysis results are in good agreement both in amplitude and in phase lag.



(a) Horizontal Disp. on the Roof (b) Horizontal Disp. in the Basement (c) Rotational Angle in the Basement
Figure 9 Comparison of Resonance Curve and Phase Lag Curve in X-direction Excitation on the Roof

5.2 Rigid Deformation and Elastic Deformation

The rigid deformation component (sway displacement and rocking displacement of the foundation) and the elastic deformation component (bending displacement and shear displacement) were segregated from the results of the forced vibration tests and the analyses, and the respective contribution of each component was analyzed. First, horizontal displacement and rotational angle at the bottom of the structure were determined, and the sway displacement and the rocking displacement that were rigid deformation component were calculated. Next, the elastic deformation component of the building model was determined as a reminder of deformation subtracting the sway displacement

and the rocking displacement from the mean displacement on each floor level. The bending displacement was calculated from the rotational angle, which was obtained from the vertical displacement of each floor level and the mean displacement according to the elastic bending theory of uniform cantilever. It was assumed that the remainder subtracting the bending displacement from the elastic deformation of the building model was the shear displacement.

Figure 10 (excitation in the X-direction) and Figure 11 (excitation in the Y-direction) show the distribution of horizontal displacement in the each level floor at the primary resonant amplitude comparing the test results and the analysis results. In the X-direction shown in Figure 10, bending displacement is very small in each case. In case 1, large shear displacement and rocking displacement on the roof in the X-direction are observed, but sway displacement on the foundation is also large due to the absence of embedment. On the other hand, in the X-direction of Cases 2 and 3 where embedment was provided, sway displacement and rocking displacement become smaller, and shear displacement was relatively significant. Shear displacement was small in the basement section where embedment was provided and was larger on the upper floor levels above the first floor. Such trends are almost the same between Case 2 and Case 3. It is also shown that the distribution of displacements in the each level floor obtained from the tests is in good agreement with the analysis results.

In the Y-direction shown in Figure 11, shear displacement as well as bending displacement were both small because the building model was designed as the rigid structure. Distribution in the Y-direction of Case 1 is in similar shape with the shape in the X-direction of Case 1 with the reduced magnitude, which clearly shows the difference between the elastic model and the rigid model. As for distribution in the Y-direction of Cases 2 and 3, the magnitude of sway displacement and rocking displacement is small because of the same effect in the X-direction, but rocking displacement is more significant because shear displacement is much smaller. Although it is a rigid model and overall displacement is small, shear displacement is small in the basement section where embedment is provided as in the case of the X-direction, and it increases at the upper floor levels above the first floor. Such trends are almost the same in Cases 2 and 3. In the analysis results, shear displacement is evaluated a little smaller on the upper floor levels above the first floor, but the analysis results are in good agreement with the test results other than the above.

When the X-direction and Y-direction are compared, because the building model in X-direction is an elastic model, elastic deformation is predominant and in Y-direction, rigid deformation is predominant because the building model in that direction is a rigid model. Such trends are clearly represented in the analysis results.

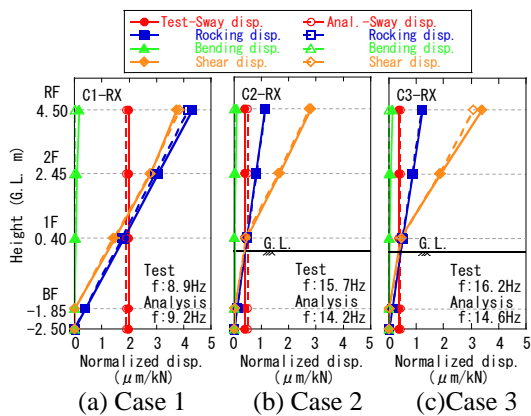


Figure 10 Comparison of Distribution of Deformation in X-direction Excitation

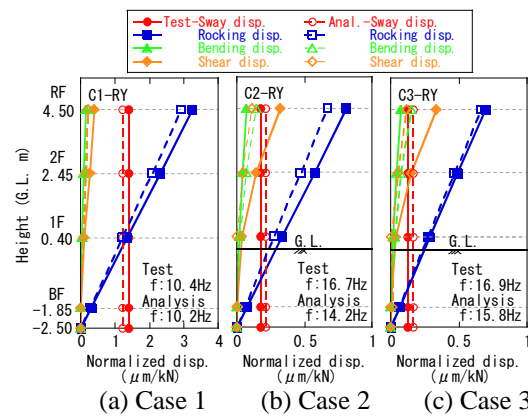


Figure 11 Comparison of Distribution of Deformation in Y-direction Excitation

5.3 Dynamic Impedance

The horizontal dynamic impedance K_{hh} was determined from the horizontal force acting at the bottom of the foundation and the horizontal displacement and the rotational dynamic impedance K_r was determined from the overturning moment and rotational angle at the bottom of foundation at each frequency based on the response on each floor level and the exciting force measured in the vibration test. Figure 12 shows the comparison between these dynamic impedance and the dynamic impedance

used in the analyses. From the test, two soil springs can be determined in the X- and Y-directions, respectively, but in the analyses only one soil spring is used because no difference is present between the directions.

In Case 1, the real part and the imaginary part of the horizontal soil spring and the rotational soil spring almost agree regardless of direction. When the test results and the analysis results are compared, the real part of the horizontal dynamic impedance from the tests tends to increase when frequency is above about 15 Hz, which is different from the trend obtained by the analyses, but in other aspects, the test results and analyses are generally in good agreement.

In cases 2 and 3, analyses could simulate the test results well except the rotational soil spring in the Y-direction. Because the slotted wall on the basement bears soil pressure in the Y-direction, it can be considered that deformation increased due to the reduced stiffness of the slotted wall. When Case 3 is compared with Case 2, the trends are generally the same in both cases, although the effect of waviness of horizontal soil spring becomes significant in the higher frequency range in the tests while waviness is observed in the analyses. When Cases 2 and 3 are compared with Case 1, the stiffness of the soil springs are apparently larger, which clearly indicates the embedment effects in the dynamic soil spring.

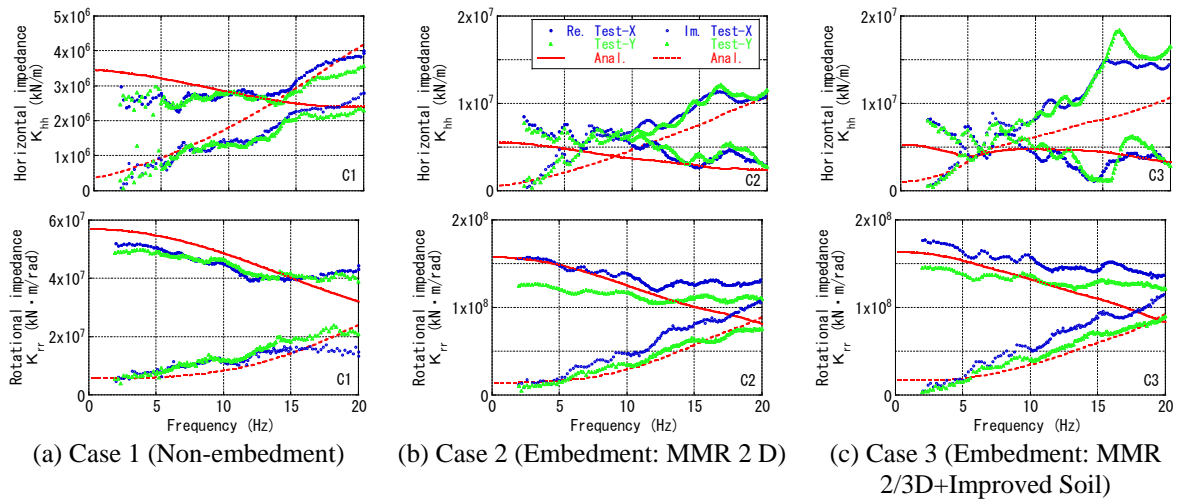


Figure 12 Comparison of the Dynamic Impedance

6. RESULTS OF VIBRATION TEST USING LARGE EXCITER

Figure 13 shows the comparison between the results of forced vibration tests using the large exciter and the small exciting force. Figure 13 (a) is a comparison of the horizontal displacement distribution in the direction of excitation on the roof, (b) is a comparison of the dynamic impedance. Because the large exciter had its own weight of about 130 kN, including jigs for installation, and its height was 0.55 m higher than that of the small exciter, direct comparison of the horizontal displacement amplitude was impossible, but the normalized amplitude on the roof in the case of intense excitation was 1.5–1.7 times larger than the amplitude in the case of moderate excitation. The primary resonant frequency indicates a shift towards the lower frequency with an increase of excitation force, which shows a effect of geometrical non-linearity. On the other hands, clear differences of the normalized amplitude are observed.

The real part and imaginary part of the horizontal soil spring in the dynamic impedance almost agree up to the frequency of about 12 Hz and to 7 Hz respectively. With respect to the real part, the results of the intensive excitation tests also almost agree at a frequency above 12 Hz. On the other hand with respect to the real part of the rotational soil spring, the value in the case of moderate excitation at 2 Hz, which is close to static loading, almost agrees with the value in the 19.6 kN excitation, but the value decreases with the increase in the excitation force, which can be considered that static spring constant is decreasing. In the case of moderate excitation, the real part gradually decreases with the increase in the frequency, but in the case of intense excitation, it rapidly decreases to the frequency of 12 Hz and the effect of non-linearity is clear. Because the rotational impedance is significantly affected by the

backfilled soil at the side, such non-linearity is considered as an effect of geometrical non-linearity between the building structure and the backfilled soil (segregation or slip), as well as non-linearity of material properties of the backfilled soil.

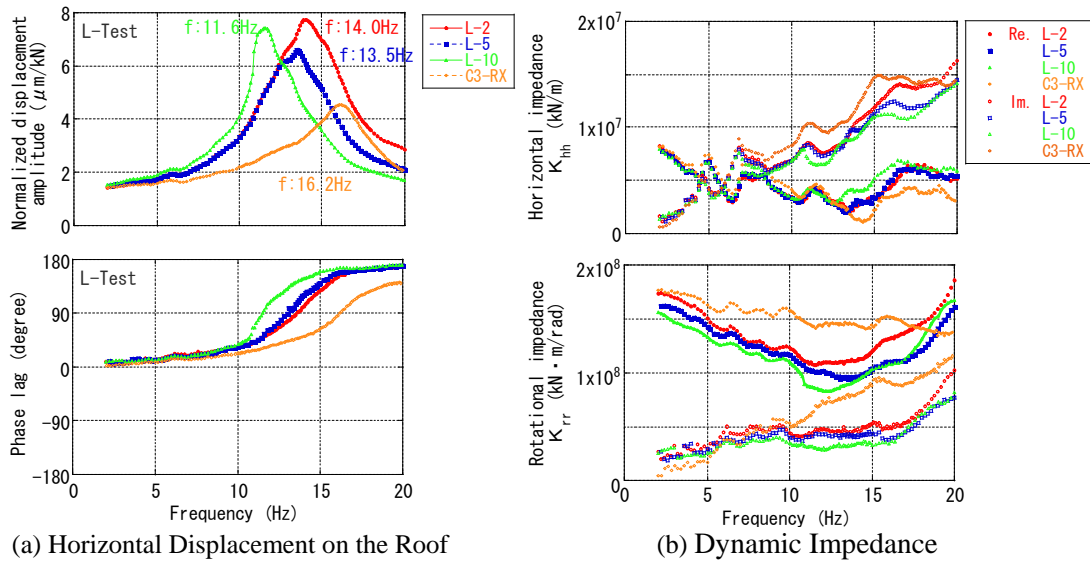


Figure 13 Comparison of Results in Intense Vibration Test

7. CONCLUSION

The forced vibration tests and the simulation analyses were conducted for the large-scaled RC building model constructed on the actual ground. The following facts were found:

- 1) Because of the embedment effects, the displacement amplitude on the roof level of the building model decreases less than half of that of Non-embedment for X: flexible direction, and less than a quarter for Y: rigid direction, respectively, compared with the result of the building model without embedment.
- 2) The response characteristics of resonance curves, the dynamic impedance, distribution of displacements, etc., are almost the same, even when MMR of outer area (farther than 2/3 of the width of the building model from surface) is replaced by improved soil.
- 3) The response characteristics, such as resonance curves, phase lag curves, dynamic impedance, etc., obtained by the tests can be reproduced by the simulation analyses in which the thin layer element model and the 3-D FEM are combined for the soil model, and the embedment effects can be evaluated using such an analysis model.
- 4) The distribution of rigid deformation (sway and rocking displacements) and elastic deformation (bending and shear deformations) in the total displacement are in good agreement between the test results and the analysis. This means the above mentioned analyses model can accurately reproduce the components of displacement.
- 5) Non-linear response of the embedded building model was observed at the intensive excitation tests conducted with larger excitation forces.

REFERENCES

- Kitada, Y., Iguchi, M., Fukuwa, N., Kusakabe, K., Nishikawa, T., Shinozaki, Y.(2001) Model Test on Dynamic Cross Interaction of Adjacent Building in Nuclear Power Plants - Overview and Outline of Earthquake Observation in the Field Test, Transactions, *SMiRT 16*, **Session K**; #1272.
- Naito, T. Yano, T., Suzuki, A., Kurita, S., Kazama, M.(2001) Model Test on Dynamic Cross Interaction of Adjacent Building in Nuclear Power Plants - Field Test, Transactions, *SMiRT 16*, **Session K**; #1138.
- Sitharam T., Sireesh S.(2005) Behavior of Embedded Footing Supported on Geogrid Cell Reinforced Foundation Beds, *SED/Geotechnical Testing Journal (GTJ)*, **Volume 28**, **Issue 5**